Proposition of a humidity control strategy for a calibrated greenhouse model with realistic controls in TRNSYS

Timothé Lalonde[1], Danielle Monfet[1], Didier Haillot[1]
[1]École de Technologie Supérieure, Montréal, Canada

Abstract

In this study the impact of different humidity control strategies on the overall energy performance of a small greenhouse was assessed. The existing greenhouse, located in Montreal, was modelled in TRNSYS and calibrated using its monthly gas consumption as well as measured indoor air temperature and relative humidity. Implementation of realistic controls for natural ventilation and for the heater were included. The greenhouse model was then used to compare four humidity control strategies: (1) natural ventilation; (2) forced ventilation with heat recovery; (3) desiccant wheel with solar and electric powered regeneration; and (4) condensation dehumidification unit.

The calibration process resulted in a model that predicted the gas consumption of the greenhouse with a CVRMSE and NMBE of 4.21% and 0.69%, respectively. The calibration of the model resulted in a RMSE of 1.65°C on the indoor air temperature. Since few details on the crops cultivated, production cycles and irrigation events were available, the calibration resulted in a high RMSE of 17.34% for the indoor air relative humidity.

When comparing the humidity control options, strategies (3) and (4) showed reduced gas energy consumption, but higher operation costs due to the electricity consumption required for air dehumidification. However, considering the energy context of Quebec, there was a reduction of greenhouse gas (GHG) emissions when using strategies (3) or (4) since electricity is mostly produced from hydroelectricity.

Introduction

In Quebec, the share of the revenue of net profits for commercial greenhouses between 2010 and 2014 was 11.2%. In Quebec, greenhouse enterprises are mostly small and 60% of the registered greenhouses with *Ministère de l'Agriculture, des Pêcheries et de l'Alimentation du Québec* (MAPAQ) have a production floor area lower than 1000 m^2, while 7% have a production floor area higher than 10,000 m^2. Smaller enterprises tend to produce over a 7-month period to reduce heating costs, while larger enterprises often produce during the whole year since they can support bigger investments to reduce operation costs.

In greenhouses, cooling and dehumidification through natural ventilation by opening roof and side vents is generally sufficient for most operating conditions (Sethi & Sharma, 2007). However, the energy costs of this strategy can be high, especially for a greenhouse operating in cold climate, since additional heating is required to maintain the temperature setpoint. Heat recovery ventilation is a strategy that is often used to reduce additional heating costs. A comparative study of simulated greenhouses located in Quebec showed that winter dehumidification through heat recovery ventilation represented 12% to 18% of the total energy consumption (de Halleux & Gauthier, 1998). Humidity control is of prime importance in greenhouses since a relative humidity below 55% or higher than 90% causes closure of the plants stomata which inhibits CO_2 absorption and growth (Hand, 1988). High relative humidity in greenhouses is also linked to increased disease risks.

The present study aims to evaluate the impacts of four different humidity control strategies on total energy consumption, energy costs and GHG emissions for a 7-month production period for a small urban greenhouse located in Montreal modelled in the building energy performance simulation software (BEPS) TRNSYS.

Greenhouse model description

The greenhouse under study (Figure 1) is a gothic arch greenhouse located in an urban area on the island of Montreal. The greenhouse is 7.62 m wide by 15.24 m long with a 3.66 m height at its centre. The greenhouse length is oriented 33° to the northeast. Rasheed, Lee, et Lee (2018) have successfully modelled a greenhouse using the multizone building model (Type 56) available in TRNSYS and this BEPS software tool is selected for this study.

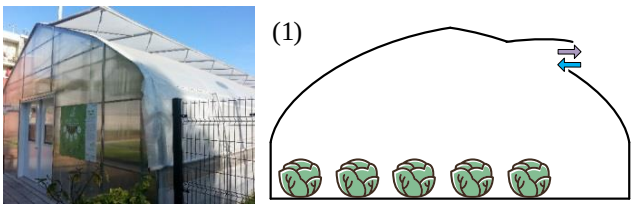

Figure 1: Modelled greenhouse

Weather data

The EPW weather data file is generated for a nearby weather station (Montreal international airport, #WMO 716270) for the year 2017. Noorian, Moradi, et Kamali (2008) have

identified that for the TRNSYS weather component Type 15, the Reindl model for tilted surface radiation computation is one of the most accurate available in TRNSYS for west-facing tilted surfaces located in the Northern hemisphere. This model is selected for tilted surface radiation calculation in this study. The simulation period is from February 24th to September 25th 2017 using a 0.005 hour simulation time step. Such a small time step is necessary due to the low thermal inertia of the greenhouse to provide adequate and stable system control responses of the proportional and on/off controllers for natural ventilation and heating system, respectively.

Envelope and structure

Using the TRNSYS3d SketchUp plugin, the geometry of the greenhouse is created as per the construction drawings of the actual greenhouse. The model includes external shading objects such as trees and adjacent buildings.

The structure is made of 3 mm thick rectangular steel braces (50 mm by 100 mm). The envelope consists of inflated double layer polyethylene on the roof and side, while the front and back facades are made of 4 mm thick polycarbonate panels.

The clear envelope materials are created in the Window 7.7 software (Mitchell et al., 2019) based on the optical and thermal properties reported for polyethylene and polycarbonate by Valera, Molina, et Alvarez (2008). According to the greenhouse plans, 95% of all the walls and roofs are covered with the clear materials. The steel structure is modelled as a resistive layer with a negligible thermal mass. The inner and outer convective heat coefficients used for double layered polyethylene and polycarbonate (H_i and H_e) are modelled according to equations 1 and 2 which were originally proposed by Watmuff, Charters, et Proctor (1977) and Garzoli et Blackwell (1987), respectively. A study by Rasheed, Lee, et Lee (2017) confirmed the accuracy of these correlations for convective heat transfer of polyethylene and polycarbonate used for greenhouse covers.

$$H_i = 1.247 \cdot (T_{ai} - T_{si})^{\frac{1}{3}} \quad (1)$$

$$H_e = 7.2 + 3.8 \cdot W_s \quad (2)$$

Where T_{ai} is the inside air temperature of the greenhouse and T_{si} is the inner cover surface temperature, both in ˚C and W_s is the wind speed in $m \cdot s^{-1}$.

The air infiltration rate in the actual greenhouse is not known. In the model, it has been set to 0.6 Air Change per Hour (ACH) as recommended by ASHRAE (2015) for greenhouses covered with plastic film.

The floor is composed of a black membrane that covers a 0.3 m thick layer of sand and gravel. The ground beneath the floor of the greenhouse is modelled with finite volume element method using TRNSYS Type 49. The exchange between the greenhouse and the ground is considered for a 5 m radius around and under the greenhouse. At the 5 m boundary, a conductive heat flux is considered with the undisturbed ground nodes. The undisturbed ground nodes temperatures are modelled as a constant deep earth temperature under the greenhouse and as a depth dependent far-field temperature on the sides of the greenhouse. The deep earth temperature is set to 10˚C and the Kusuda-Achenbach model (Kusuda & Achenbach, 1965) is used to estimate the temperature of the undisturbed ground at the far-field boundary condition in function of the depth of the node and thermal properties of the ground.

Internal loads

In the greenhouse, it is assumed there is an average of five people doing light work from 6:00-18:00 on weekdays. This is modelled using the TRNSYS standard library (Klein et al., 2017) for a degree of activity V (standing, light work and walking in a 24˚C environment). Three lights are installed inside the greenhouse to improve visibility and are only occasionally lit. The internal load caused by the lights is considered negligible.

Four horizontal circulation fans are used inside the greenhouse to maintain well-mixed air conditions and limit the effect of stratification. The convective heat gain from fan operation is 54 W per fan.

Finally, the crops are cultivated in elevated grow beds inside the greenhouse. During the period under study these crops are mostly leafy greens. It is assumed that an average of 40% of the greenhouse floor area is covered by the elevated grow beds during this period. The cultivation period ranges from March 24th to September 25th. A crop model is used to estimate the rates of heat gain/loss (sensible and latent) induced by crops. The TRNSYS Type proposed by Talbot et Monfet (2020) for lettuce, which is based on equations proposed by Graamans, van den Dobbelsteen, Meinen, et Stanghellini (2017), is used. The rates of heat gain/loss induced by crops vary according to the photoactive radiation (PAR), the indoor air temperature and relative humidity as well as parameters that define the crop production. These parameters are the greenhouse floor area in m^2; the cultivated density (CD), which represents the fraction of the cultivated area over the floor area; the leaf area index (LAI), which represents the average ratio of leaf area over the cultivated area; and the canopy area coverage (CAC), which indicates the percentage of the cultivated area completely covered by the canopy.

This crop model is modified (1) to use transmitted solar radiation to the zone rather than artificial light power for calculation of available PAR and (2) to calculate the PAR absorbed by the plants and remove it from the total radiation used in the heat balance calculation of the greenhouse model.

The CD of the crop (lettuce) model is set to 40%. The LAI of the lettuces is set to 3 and the CAC is set to 80% based on the relationship between the LAI and CAC for lettuce proposed by Tei, Scaife, et Aikman (1996). Figure 2

presents the interactions between the greenhouse model and the crop (lettuce) model.

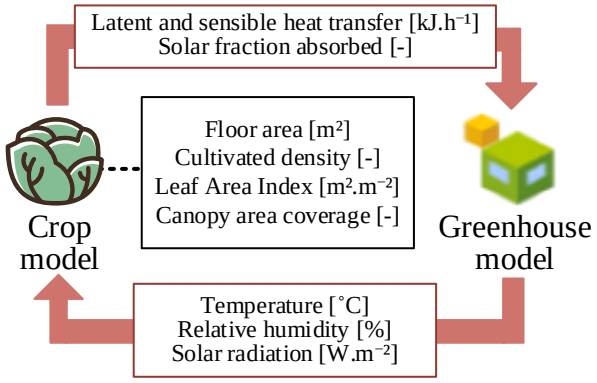

Figure 2: Inputs and outputs of the lettuce model

Equipment and controls

The natural gas unit heater is modelled in TRNSYS using Type 663 with a heating capacity of 48.93 kW, a thermal efficiency of 93% and an air flow rate of 1425 L·s^{-1}, as installed in the actual greenhouse. A calorific value of 37890 kJ·m^{-3} is used to convert the fuel consumption heat rate to cubic metres of natural gas consumption as used by the natural gas utility provider (Energir, 2018).

Natural ventilation is used to cool the air inside the greenhouse through a 7.5 m^2 roof vent opening. Two 15 m^2 side vents can also be opened manually when the greenhouse is overheating. A simplified ventilation model is selected to model the air flow rate entering the greenhouse through the vents. This model uses a design air flow rate which is influenced by environmental conditions such as the difference between indoor and outdoor temperatures and the wind speed as described by equation 3 (Coblentz & Achenbach, 1963).

$$\dot{V} = \dot{V}_d \cdot OF \cdot (A + B \cdot |T_{ai} - T_{odb}| + C \cdot W_s + D \cdot {W_s}^2) \quad (3)$$

Where $\dot{V}$ is the calculated air flow rate in m^3·s^{-1}; $\dot{V}_d$ the design air flow rate in m^3·s^{-1}; OF the opening factor of the window; A is a user-defined constant; B is a coefficient influenced by the temperature difference; and C and D are coefficients influenced by the wind speed. EnergyPlus documentation (Crawley et al., 2018) recommends values for these parameters of 0.606, 0.03636, 0.1177 and 0, respectively.

The wind speed at the weather station is taken at a height of 10 m. It is necessary to correct this value for a 3 m height, which is the centre height of the greenhouse roof vent. This is achieved using the wind profile power law equation (equation 4).

$$W_s = W_s' \cdot \left(\frac{H}{H'}\right)^{\alpha} \quad (4)$$

Where W_s is the corrected wind speed in m·s^{-1}; W_s' the measured wind speed in m·s^{-1}; H the height of the vent in m; H' the height of the weather station pylon in m and α an empirically derived coefficient with a value of 1/7 (Manwell, McGowan, & Rogers, 2010).

The design air flow rate is estimated as per equation 5, which is defined in the CIBSE application manual (2005) for a single cell model.

$$\dot{V}_d = C_d \cdot A_i \cdot \sqrt{\frac{2 \cdot |\Delta p_i|}{\rho}} \quad (5)$$

Where C_d is the discharge coefficient of the opening; A_i the area of the opening in m^2; Δp_i the pressure difference between indoor and outdoor conditions in Pa and ρ the air density in kg·m^{-3}.

In order to model the design air flow rate in the most critical conditions, it is common practice to calculate Δp_i for a temperature difference of 3˚C and in the absence of any wind effect (CIBSE, 2005). In the greenhouse model, only the roof vent is considered since the side vents are manually operated. A typical C_d value of 0.6 is used in this case as suggested in the TRNSYS documentation (Klein et al., 2017).

The controls for heating and ventilation use an IGrow 800 controller with a single on/off control stage (H1) for the heater and six proportional control stages (C1 to C6) for ventilation. The ventilation stages control the opening of the roof vent when the temperature rises above the low limit of each stage. Table 1 presents the control strategy in place in the actual greenhouse. No humidity control strategy is used at this point. Until March 7th the heating setpoint is set to 14˚C.

Table 1: Controller settings

Heating stage	**Heater setpoint (day/night)**	**Period used**
H1 winter	18.5˚C/18˚C	07/03 – 06/06
H1 summer	17.5˚C/15˚C	06/06 – 25/09
Cooling stage	**Cooling stage limits (low/high)**	**Roof vent opening**
C1	22.5˚C/23.5˚C	15%
C2	23.5˚C/24.5˚C	35%
C3	24.5˚C/25.5˚C	55%
C4	25.5˚C/26.5˚C	70%
C5	26.5˚C/27.5˚C	85%
C6	27.5˚C/28.5˚C	100%

The TRNSYS Type 974 controller with a minimum stage runtime of 5 minutes, low temperature dead band of 0.5°C and high temperature dead band of 3.5°C is used to model the heater control stage (H1), while TRNSYS Type 1669, a proportional controller, is used to control the roof vent opening factor as detailed in Table 1. A delay of one time step on the greenhouse air temperature and relative humidity, modelled using TRNSYS Type 661, was imposed on the input to the controller to improve the stability of the simulation. To prevent cycling, a delay of 5 minutes before switching stages is used.

Model calibration

The model is calibrated for the gas consumption, which is compiled monthly by the gas provider in cubic metres. The model is also calibrated for the indoor air temperature and for the relative humidity, which are recorded every 10 seconds with a precision of ±0,3˚C and ±3%, respectively. The approach for calibrating the model follows the guidelines proposed by Sun et Reddy (2006). The first step in this approach is identifying all the possible calibration parameters in the model. In order to determine the reliability of the initial value given to these parameters, the approach proposed by Raftery, Keane, et O'Donnell (2011) is used. This approach is based on the use of reliability indexes of the source, as listed below. A low index represents a parameter of higher reliability.

1. Data-logged measured data;
2. Spot or short term measured data;
3. Direct observation on site;
4. Operator and personnel survey;
5. Operation documents;
6. Commissioning documents;
7. Benchmark studies;
8. Standards, specification and best practice guides;
9. Design stage information.

Table 2 presents all the identified parameters, their initial values in the reference model, their priority index and reliability index. The priority indexes are those proposed by Sun et Reddy (2006): 1) building envelope; 2) systems schedule; 3) internal gains schedule; 4) internal gains and 5) system variables. Also, in this study, parameters with a reliability index of 4 or lower (parameters marked with an asterisk in Table 2) are considered sufficiently reliable and are fixed to their initial value.

A sensitivity analysis is conducted over the remaining parameters. The sensitivity analysis allows identifying the parameters of higher influence in order to further reduce the number of parameters to be calibrated. Equation 6, as proposed by Lam et Hui (1996), is used to calculate the sensitivity coefficient (SC). Higher SC indicates higher influence of a modification of the input on the output of interest.

$$SC = \frac{(OP_m - OP_{bc})/OP_{bc}}{(IP_m - IP_{bc})/IP_{bc}} \quad (6)$$

Where SC represents the sensitivity coefficient; OP_m an output of interest of the simulation with the modified value of the studied parameter; OP_{bc} the same output of the simulation with the initial value of the studied parameter; IP_m the modified value of the studied parameter and IP_{bc} the initial value of the studied parameter.

Following the sensitivity analysis, the number of parameters to be calibrated is reduced to five parameters, as presented in Table 3, where the range of variation and the increment used during the calibration for each parameter is also specified.

Table 2: Reliability and priority of the identified parameters

Parameter	Base case	Reliability index	Priority index
PC conductivity	0.19 $W \cdot m^{-1} \cdot K^{-1}$	7	1
PC solar/visible transmittance	0.78	7	1
PC infrared emissivity	0.96	7	1
PE conductivity	0.45 $W \cdot m^{-1} \cdot K^{-1}$	7	1
PE solar/visible transmittance	0.91	7	1
PE infrared emissivity	0.84	7	1
Fenestration	95%	3*	1
Ground density	2500 $kg \cdot m^{-3}$	7	1
Ground conductivity	0.7 $W \cdot m^{-1} \cdot K^{-1}$	7	1
Ground specific heat	1 $kJ \cdot kg^{-1} \cdot K^{-1}$	7	1
Nb of occupants	5 occupants	4*	4
Occupation schedule	Weekdays, 6:00-18:00	4*	3
Fan heat gains	216 W	4*	4
Fan schedule	Every day	4*	3
Infiltration rate	0,6 ACH	8	1
Ventilation design flow rate	2,7 $m^3 \cdot s^{-1}$	7	5
Floor solar absorptance	0.9	7	1
Cultivated density	0.4	9	4

Table 3: Calibration parameters

Parameter (first to last)	Range	Increment
PE solar/visible transmittance	0.85-0.91	0.01
Floor solar absorptance	0.7-0.9	0.02
Infiltration rate	0.5-1.2	0.1
PE infrared emissivity	0.78-0.84	0.01
Cultivated density	0.2-0.5	0.1

The performance of the model is evaluated with the coefficient of variance of the root mean square error (CVRMSE) of the monthly gas consumption, the normalized mean bias error on the monthly gas consumption (NMBE), the root mean square error (RMSE) and the coefficient of determination (R^2) of the hourly temperature and relative humidity. Equations 7, 8, 9 and 10 present the calculation of these four statistical indicators.

$$RMSE = \sqrt{\frac{\sum(D_{m.i} - D_{s.i})^2}{n}} \quad (7)$$

$$NMBE(\%) = \frac{\sum(D_{m.i} - D_{s.i})}{\sum(D_{m.i})} \cdot 100 \quad (8)$$

$$CVRMSE = \frac{RMSE}{D_{m.avg}} \cdot 100 \quad (9)$$

$$R^2 = 1 - \frac{\sum(D_{m.i} - D_{s.i})^2}{\sum(D_{m.i} - D_{m.avg})^2} \quad (10)$$

Where $D_{m.i}$ indicates the measured data point i; $D_{s.i}$ the simulated data point i; n the number of data pairs and $D_{m.avg}$ the measured data points average.

Since the temperature and humidity measurements are recorded every 10 seconds, these measurements are averaged over an hour to obtain the hourly measured data.

A MATLAB script modifies each of the parameters over its range of variation, launches the simulations and analyses the results. A combined index is used to evaluate the calibration of the model based on its ability to adequately predict monthly gas consumption, hourly temperature and relative humidity. Additionally, the gas consumption NMBE must be lower than ±5% and the R^2 on temperature higher than 0.75, as per ASHRAE (2017).

Table 4 presents the results of the calibration process for the greenhouse model. The six statistical indicators of interest are displayed for both the initial model and the calibrated model.

Table 4 : Calibration results

Output	Indicator	Initial	Calibrated
Gas consumption [$m^3.month^{-1}$]	CVRMSE	9.35 %	4.21 %
	NMBE	6.48 %	0.69 %
Temperature [°C]	RMSE	1.84°C	1.65°C
	R^2	0.78	0.83
Relative humidity [%]	RMSE	17.63	17.34
	R^2	0.20	0.23

ASHRAE guideline 14 (2017) requires 12 months of data to complete the calibration; due to the context of the study, monthly gas consumption data is only available for 7 months (from February to September). For that period, the calibration results show that the monthly heating energy consumption is within the criteria established by ASHRAE guideline 14 (2017) with a CVRMSE and NMBE lower than 15% and ±5%, respectively.

The calibration results show little improvement for the temperature and relative humidity: the RMSE and R^2 are similar for the base case and the final model and are higher than the absolute precision of the temperature sensor of 0.6˚C and of the relative humidity sensor of 6%. This can be explained by the fact that in TRNSYS the zone is considered as a single well-mixed air node while in reality it takes time for the air to mix properly. This causes a delay in the measured air temperature response compared to the results of the simulation.

Figure 3 and Figure 4 show the measured and predicted temperature and relative humidity profiles on June 23rd, 2017. The shaded area represents the uncertainty range of the sensor used to measure temperature and relative humidity. No measurement is made for absolute humidity, which is obtained as a function of temperature and relative humidity.

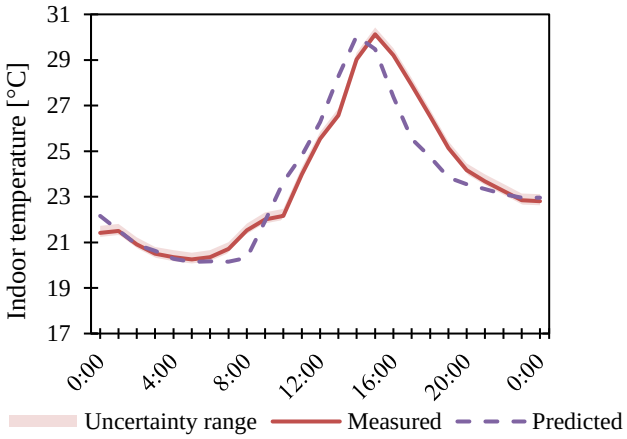

Figure 3 : Measured and predicted temperature profile on June 23rd, 2017

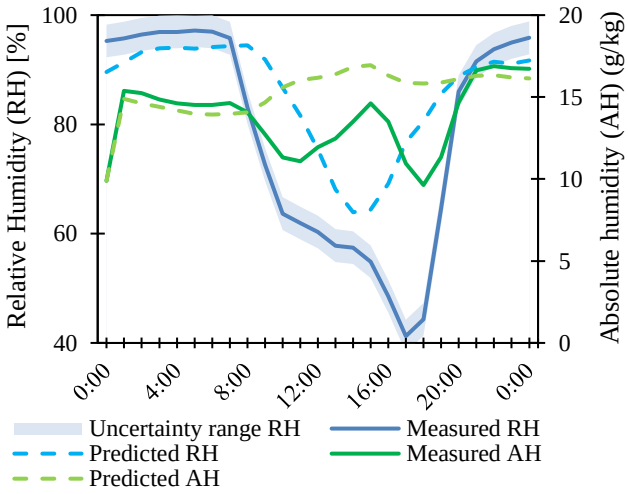

Figure 4 : Measured and predicted humidity profile on June 23rd, 2017

For the temperature profile (Figure 3), some thermal mass elements have been neglected, such as the steel structure and elevated grow beds inside the greenhouse. This could explain the phase shift in temperature for the model.

The relative humidity cannot be properly predicted by the model. Our hypothesis is that it is caused by the crop modelling approach that: (1) does not model the crop growth, which can lead to overestimated or underestimated rates of heat gain/loss induced by crops during germinating and when the crops are mature, respectively; (2) only models leafy greens, which is not the only crop type being cultivated and might not be representative of fruit crops such as tomatoes, (3) does not take into account soil evaporation caused by excess irrigation; (4) calculates the evapotranspiration rate of a plant which is never subjected to any water stress, which is difficult to achieve in real life operation of the greenhouse since irrigation events are irregular.

As illustrated on Figure 4, the difference between the measured and predicted relative humidity in the greenhouse

is larger during the photoperiod where evapotranspiration rates are the most important and operators are present inside the greenhouse to water crops. The accuracy of the natural ventilation model used and differences between the local weather conditions and those measured at the weather station could also explain these results.

These discrepancies do not allow us to use this model to make prediction on the relative humidity within the greenhouse. However, it can be used to compare different humidity control strategies using the same input parameters to provide insight on their impact on the energy consumption of the greenhouse.

Humidity control strategies

Four humidity control strategies are compared: (1) natural ventilation (as illustrated in Figure 1); (2) forced ventilation with heat recovery; (3) desiccant wheel with solar and electric powered regeneration; and (4) condensation dehumidification unit (all illustrated in Figure 5). Each strategy is simulated over a 7-month operation period from March 1st to October 1st. In all scenarios, the relative humidity setpoint is set to 80% ±3% as proposed by the greenhouse operator. For strategies (2) to (4), the systems are used only during the spring and autumn months when the roof vent is closed, while natural ventilation is used for dehumidification from June to September. It is assumed that the base electricity consumption (lights, small appliances, etc.) would remain the same in all scenarios. Only electricity consumption linked to the heating and dehumidification systems are considered for comparison purposes.

Systems modelling

Strategy (1) uses a proportional controller (Type 1669 in TRNSYS) to control the opening of the roof vent proportionally if the relative humidity rises above 77% to a maximum roof vent opening of 15% when the relative humidity rises to 83%. The electricity consumption for this strategy is the power drawn by the heater's blower. The power consumed by the roof vent actuator is negligible.

Strategy (2) uses a heat recovery ventilation system (HRV) to force the evacuation of humid air. Heat recovery is done using a heat exchanger with an average sensible effectiveness of 40% to consider the effects of clogging and defrosting (Jorgenson, 1989). The power drawn by this equipment is 0.1 kW and the rated air flow rate is 90 $L \cdot s^{-1}$. The electricity consumption for this strategy is the power drawn by the HRV system plus the electric consumption of the heater's blower.

Strategy (3) is an exploratory design based on an outdoor air solid desiccant dehumidification system. This system uses a hygroscopic material, silica gel, to dehumidify and heat the supply air. The hygroscopic material is regenerated by forcing the passage of high temperature air through it. In this case, the regeneration air comes from the greenhouse exhaust air that passes through a 1 m^2 solar thermal collector facing south with a slope of 45° and a 1.5 kW electric heating coil. The fans, desiccant and heat recovery wheels together drawn 0.3 kW when operating. The rated process air flow rate is 70 $L \cdot s^{-1}$, while the regeneration air flow rate is 26 $L \cdot s^{-1}$. The desiccant wheel is modelled using Type 1225. The electric heating coil is modelled using Type 930 and the regeneration air temperature setpoint for the coil is set to 100°C. The solar collector is modelled as a flat plate air heating collector (Type 561). The electricity consumption for this strategy is the sum of the power drawn by the fan, wheel and heating coil.

Strategy (4) uses a condensation dehumidification unit. A heat exchanger reduces the cooling coil and reheating coil demands by precooling intake air with the supply air. Fan and compressor waste heat are added to the supply air stream. This is modelled using the unitary dehumidifier Type 688 in TRNSYS with a rated flow rate of 92 $L \cdot s^{-1}$ and fan power of 0.1 kW. The electricity consumption of this strategy is equal to the sum of the dehumidifier fan, the dehumidifier compressor and heater's blower power consumption.

Results

The gas and electricity consumption of all the tested strategies is presented in Figure 6 and Figure 7, respectively. For strategy (1), introducing humidity control through natural ventilation in the model resulted in a 24% increase in gas consumption compared to the reference model (without ventilation control for dehumidification). For strategy (2), the gas consumption is 11% higher compared to the reference model, which is consistent with an increase of 12% reported by de Halleux et Gauthier (1998) for the same type of system over a period ranging from September to May for a greenhouse in Quebec climate.

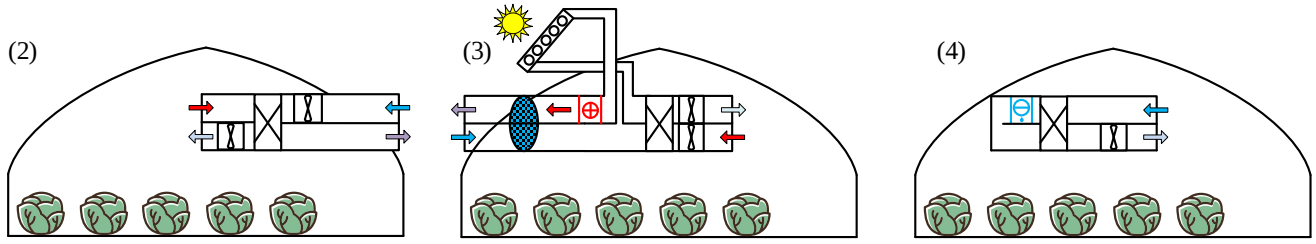

Figure 5 : Systems installed to assess the proposed humidity control strategies (2) forced ventilation with heat recovery; (3) desiccant wheel with solar and electric powered regeneration; and (4) condensation dehumidification unit

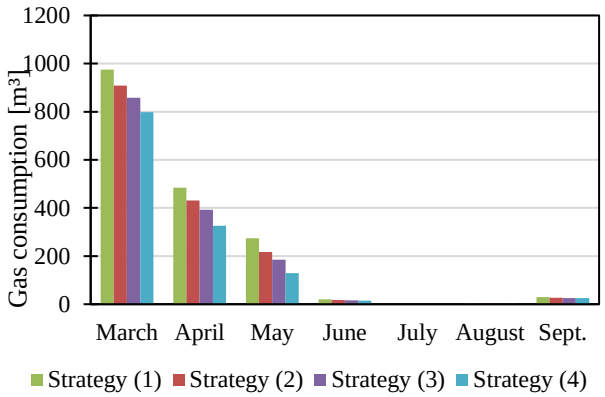

Figure 6 : Gas consumption for humidity control strategies (1), (2), (3) and (4)

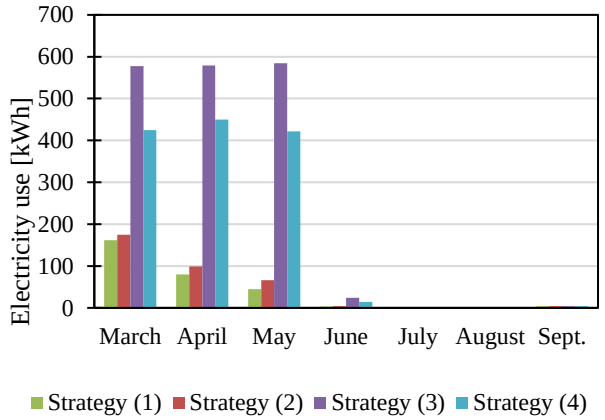

Figure 7 : Electricity consumption for humidity control strategies (1), (2), (3) and (4)

Strategies (3) and (4) allow for reductions of 17% and 27% of the total gas consumption respectively compared to the use of natural ventilation as a dehumidification (strategy (1)), with an important increase in electricity consumption. The energy consumption of strategies (2) (3) and (4) could potentially be further reduced using a proportional controller instead of an on/off controller. The addition of the solar panel does not have a significant impact on electricity consumption of the regeneration heating coil since most of the dehumidification load occurred at night. One advantage of strategy (4) is that it can be used to control humidity even if the outside air is warm and humid, which could result in higher yields during the summer months. A greenhouse operator searching for the best dehumidification strategy will have to bear in mind the energy production context in which he/she is located.

The operation costs and equivalent GHG emissions over the production period of March to October are presented in Table 5. The costs are calculated using Énergir (formerly Gaz Metro) 2017 rates for natural gas and the Hydro-Quebec rate D for electricity. The Hydro-Quebec D rate does not account for peak demand charge.

Table 5 : Costs and GHG emissions from March 1st to October 1st for the four humidity control strategies

	Costs [$]	**GHG emissions [kg CO_2 eq]**
Strategy (1)	299.90	3321.69
Strategy (2)	277.05	2986.02
Strategy (3)	390.42	2755.29
Strategy (4)	319.90	2416.52

Strategies (3) and (4) have higher operation costs over a 7-month period than the strategies relying on ventilation like strategy (1) and strategy (2). Strategies (3) and (4) however consume less gas for heating which results in reduced GHG emissions considering Quebec's energy production context.

Conclusion

The aims of this study were twosome: (1) to calibrate a TRNSYS greenhouse model and (2) to compare four different humidity control strategies on gas and electricity consumption and associated costs and GHG emissions. The modelled greenhouse, located in Montreal, included detailed systems and controls as well as a lettuce model to estimate the rates of heat gain/loss (sensible and latent) induced by crops.

The results of the calibration process highlighted the difficulty to calibrate a greenhouse model with low thermal inertia and the importance of adequately modelling the crop production and irrigation cycles. An enhanced calibration method for greenhouses is proposed for future work. Locally measured weather data should be used if available for calibration. The first step of this approach would require calibrating the greenhouse model envelope characteristics and available solar energy inside the greenhouse during a period where no crops are cultivated and no ventilation, irrigation or heating systems are used inside the greenhouse. This would allow to calibrate the properties of the envelope and the thermal inertia of the greenhouse. Calibrating available PAR radiation inside the greenhouse is of prime importance since it has an important impact on modelled crop evapotranspiration rates. The second step would be to calibrate the model without crops but with the natural ventilation and heating systems. The third and last step would be to integrate the crop model and irrigation events to estimate the sensible and latent heat transfer induced by crop production. For this last step, calibration should occur for a period of constant production and might require calibration of parameters such as the CD and LAI.

This study also highlights the impact of humidity control on the total energy consumption of a greenhouse in cold climate. The humidity control strategy that showed the most potential to reduce operation costs is strategy (2), forced ventilation with heat recovery fans. The model implementing this strategy showed similar results to those reported by de Halleux et Gauthier (1998) and Campen, Bot, et De Zwart (2003). Due to Quebec's electricity production being mainly hydroelectric, strategies (3) and (4) led to

lower GHG emissions. For a 7-month production period, it might not be worth investing in additional systems to provide humidity control of the greenhouse. However, for larger greenhouses operating year-round, the return on investment of strategy (2) could be interesting since the savings during the winter months are more important.

References

ASHRAE. (2015). ASHRAE Handbook - HVAC Applications (SI Edition). Atlanta: American Society of Heating, Refrigerating and Air-Conditioning Engineers, Inc. (ASHRAE).

ASHRAE. (2017). ASHRAE Handbook - Fundamentals (SI Edition). Atlanta: American Society of Heating, Refrigerating and Air-Conditioning Engineers, Inc. (ASHRAE).

Campen, J., Bot, G., & De Zwart, H. (2003). Dehumidification of greenhouses at northern latitudes. *Biosystems Engineering, 86*(4), 487-493.

CIBSE. (2005). 4.2.1.1 Basic Equations for an Opening. In *Natural Ventilation in Non-Domestic Buildings - CIBSE Applications Manual AM10*. CIBSE.

Coblentz, C., & Achenbach, P. (1963). Field measurements of air infiltration in ten electrically-heated houses. *Ashrae Transactions, 69*(1).

Crawley, D. B. et al. (2018). EnergyPlus 8.9.0 documentation : Engineering reference. Washington D.C., U.S.A. : U.S. Department of Energy.

de Halleux, D., & Gauthier, L. (1998). Energy Consumption Due to Dehumidification of Greenhouses under Northern Latitudes. *Journal of agricultural engineering research, 69*(1), 35-42.

Energir. (2018). Technical properties of natural gas supply in Quebec. Montreal, QC, CA: Energir.

Garzoli, K. V., & Blackwell, J. (1987). An analysis of the nocturnal heat loss from a double skin plastic greenhouse. *Journal of agricultural engineering research, 36*(2), 75-86.

Graamans, L., van den Dobbelsteen, A., Meinen, E., & Stanghellini, C. (2017). Plant factories; crop transpiration and energy balance. *Agricultural Systems, 153*, 138-147.

Hand, D. W. (1988). Effects of atmospheric humidity on greenhouse crops. Acta Horticulturae 229. 143-158.

Jorgenson, M. E. & May D. (1989). *Demonstration of heat recovery ventilators in livestock housing.* Portage la Prairie, MB, Canada: Prairie agricultural machinery institue.

Klein, S. et al. (2017). TRNSYS 18: A transient system simulation program. Madison, WI, USA: Solar Energy Laboratory, University of Wisconsin.

Kusuda, T., & Achenbach, P. R. (1965). Earth temperatures and thermal diffusivity at selected stations in the United States. *Ashrae Transactions, 71*(1), 61-74.

Lam, J. C., & Hui, S. C. (1996). Sensitivity analysis of energy performance of office buildings. *Building and environment, 31*(1), 27-39.

Manwell, J. F., McGowan, J. G., & Rogers, A. L. (2010). *Wind energy explained: theory, design and application*. John Wiley & Sons.

Mitchell, R. K., C. Curcija, D., Zhu, L., Vidanovic, S., Czarnecki, S., Arasteh, D., Carmodi, J., & Huizenga, C. (2019). Window 7.7. Berkeley, CA, USA: Lawrence Berkeley National Laboratory.

Noorian, A. M., Moradi, I., & Kamali, G. A. (2008). Evaluation of 12 models to estimate hourly diffuse irradiation on inclined surfaces. *Renewable Energy, 33*(6), 1406-1412.

Raftery, P., Keane, M., & O'Donnell, J. (2011). Calibrating whole building energy models: An evidence-based methodology. *Energy and Buildings, 43*(9), 2356-2364.

Rasheed, A., Lee, J., & Lee, H. (2018). Development and optimization of a building energy simulation model to study the effect of greenhouse design parameters. *Energies, 11*(8), 19.

Rasheed, A., Lee, J. W., & Lee, H. W. (2017). Development of a model to calculate the overall heat transfer coefficient of greenhouse covers. *Spanish journal of agricultural research, 15*(4), 11.

Sethi, V., & Sharma, S. (2007). Survey of cooling technologies for worldwide agricultural greenhouse applications. *Solar Energy, 81*(12), 1447-1459.

Sun, J., & Reddy, T. A. (2006). Calibration of building energy simulation programs using the analytic optimization approach (RP-1051). *HVAC&R Research, 12*(1), 177-196.

Talbot, M.-H., & Monfet, D. (2020). Estimating the impact of crops on peak loads of a Building-Integrated Agriculture space. *Science and Technology for the Built Environment, 26*(10), 1448-1460.

Tei, F., Scaife, A., & Aikman, D. (1996). Growth of lettuce, onion, and red beet. 1. Growth analysis, light interception, and radiation use efficiency. *Annals of Botany, 78*(5), 633-643.

Valera, M., Molina, A., & Alvarez, M. (2008). *Protocolo de auditoría energética en invernaderos*. Madrid, Spain: IDAE.

Watmuff, J., Charters, W., & Proctor, D. (1977). Solar and wind induced external coefficients - Solar collectors. *Cooperation Mediterraneenne pour l'Energie Solaire 1*. 56.